

# Microwave-Assisted One-Step Synthesis of Polyacrylamide–Metal (M = Ag, Pt, Cu) Nanocomposites in Ethylene Glycol

Jie-Fang Zhu and Ying-Jie Zhu\*

State Key Laboratory of High Performance Ceramics and Superfine Microstructure, Shanghai Institute of Ceramics, Chinese Academy of Sciences, Shanghai 200050, People's Republic of China

Received: January 24, 2006; In Final Form: March 10, 2006

Polyacrylamide–metal (M = Pt, Ag, Cu) nanocomposites with metal nanoparticles homogeneously dispersed in the polymer matrix have been successfully prepared with the corresponding metal salt and acrylamide monomer in ethylene glycol by microwave heating. This method is based on the single-step simultaneous formation of metal nanoparticles and polymerization of the acrylamide monomer, leading to a homogeneous distribution of metal nanoparticles in the polyacrylamide matrix. Ethylene glycol acts as both a reducing reagent and a solvent, thus no additional reductant is needed. Another advantage is that no initiator for AM polymerization and no surfactant for stabilization of metal nanoparticles are necessary. The products were characterized by X-ray powder diffraction (XRD), transmission electron microscopy (TEM), Fourier transform infrared (FTIR), ultraviolet visible (UV–vis) absorption spectra, and thermogravimetric (TG) and differential scanning calorimetric analysis (DSC).

## Introduction

Polymer–metal nanocomposites have recently received much attention due to their intriguing optical, electrical, and mechanical properties. These nanocomposites are considered to be interesting functional materials with wide potential applications in various fields.<sup>1–6</sup> To develop simple, fast, low-cost methods for synthesis of these nanocomposites is very important for realizing their large-scale production and applications.

Successful synthesis of high-performance nanocomposites depends on good control over nanocrystallite size, size distribution, and dispersity. A number of methods have been developed to synthesize polymer–metal nanocomposites. Conventionally, polymerization of the organic monomer and formation of metal particles were conducted separately, leading to the inhomogeneous mixing of the polymer and metal particles and aggregation of metal particles, which created the uneven properties in the composites. In some preparation methods, relatively high temperatures or pressures were needed, which made the preparation complex, difficult, and high-cost. Nanocomposites were also synthesized by the preparation of metal nanoparticles in situ, while the pre-prepared polymer was present during preparation of metal nanoparticles or added afterward.<sup>7</sup> Finally, the nanocomposites were obtained from the dispersion of nanoparticles in polymer solution by solvent evaporation or coprecipitation. In these methods, metal nanoparticles were formed by the reduction of metal ions with a reductant or heating treatment.<sup>8–11</sup> There have been only a few reports on one-step simultaneous formation of metal nanoparticles and polymerization of the monomer. For example, the  $\gamma$ -irradiation method and the ultraviolet irradiation technique were applied to synthesize polymer–metal nanocomposites, in which the reduction of metal ions and the polymerization of the monomer were simultaneous.<sup>12–14</sup> Polyacrylonitrile–silver nanocomposite was synthesized by a simultaneous polymerization and reduction

process in the presence of the initiator of 2,2-azobis(isobutyronitrile) under the protection of nitrogen; however, a heating time of 10 h was needed in the preparation.<sup>15</sup> Unfortunately, these methods are limited for commercial applications due to the availability of the  $\gamma$ -ray source or relatively long preparation time.

The application of microwave heating in synthetic chemistry is a fast growing research area.<sup>16–18</sup> Since the first reports of microwave-assisted synthesis in 1986, the microwave heating has been accepted as a promising method for rapid volumetric heating, higher reaction rate and selectivity, reducing reaction time often by orders of magnitude, and increasing yield of products compared to conventional heating methods. This has opened up the possibility of realizing new reactions in a very short time. However, application of microwave chemistry to the one-step simultaneous synthesis of polymer–metal nanocomposites has been little exploited despite these advantages.

In this study, we report the fast microwave-assisted synthesis of polyacrylamide–metal (M = Ag, Pt, Cu) nanocomposites with metal nanoparticles homogeneously dispersed in the polymer matrix using corresponding metal salt and acrylamide monomer in ethylene glycol. This method is based on the single-step simultaneous formation of metal nanoparticles and polymerization of the acrylamide monomer, leading to a homogeneous distribution of metal nanoparticles in polyacrylamide matrix. Ethylene glycol acts as both a reducing reagent and a solvent, thus no additional reductant is needed. Another advantage is that no initiator for acrylamide polymerization and the surfactant for stabilization of metal nanoparticles are needed. This makes it possible to avoid subsequent complicated workup procedures for removal of these additives, leading to speed, simplicity, and low-cost in the preparation of polymer–metal nanocomposites.

## Experimental Section

Chemicals used in the experiments were analytical grade reagents and were used without further purification. In a typical

\* To whom any correspondence should be addressed. E-mail: y.j.zhu@mail.sic.ac.cn. Phone: +86-21-52412616. Fax: +86-21-52413122.

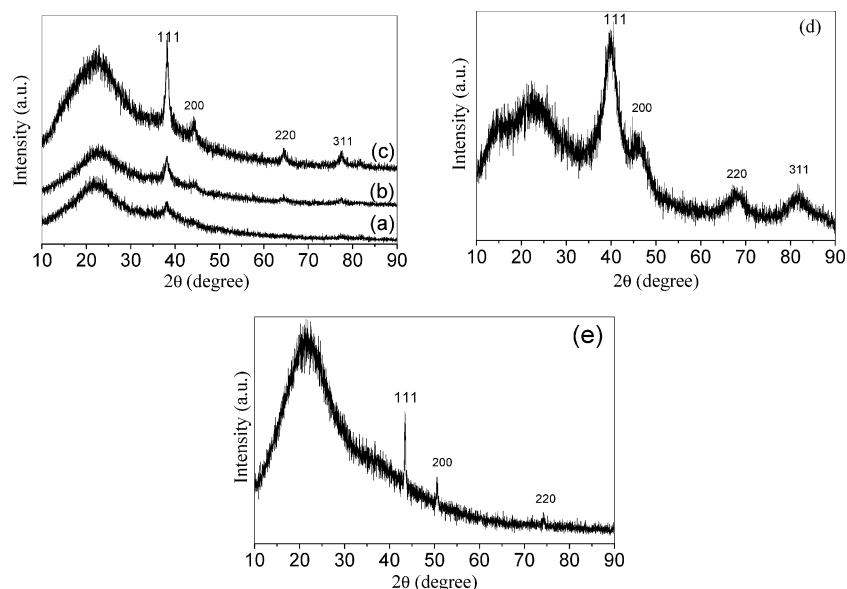


**Figure 1.** (a–c) XRD patterns of PAM–Ag nanocomposite prepared by microwave heating the EG solution of 0.01 M  $\text{AgNO}_3$  and 3 M AM at different temperatures for 15 min: (a) 125, (b) 150, and (c) 190 °C. (d) XRD pattern of PAM–Pt nanocomposite prepared by microwave heating the EG solution of 0.01 M  $\text{K}_2\text{PtCl}_6 \cdot 6\text{H}_2\text{O}$  and 3 M AM at 180 °C for 15 min. (e) XRD pattern of PAM–Cu nanocomposite prepared by microwave heating the EG solution of 0.01 M  $\text{CuSO}_4 \cdot 5\text{H}_2\text{O}$  and 3 M AM at 197 °C for 15 min.

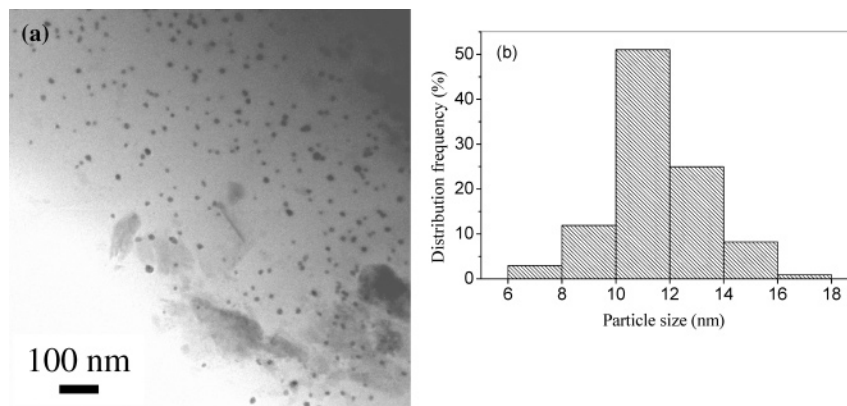
procedure, the appropriate amount of metal salt ( $\text{AgNO}_3$ ,  $\text{K}_2\text{PtCl}_6 \cdot 6\text{H}_2\text{O}$ , or  $\text{CuSO}_4 \cdot 5\text{H}_2\text{O}$ ) and 10.662 g of acrylamide (AM) were dissolved in 50 mL of ethylene glycol (EG) under magnetic stirring. The solution was rapidly microwave-heated to a given temperature, and kept at this temperature for a given time. The details of the amount of metal salt, the reaction temperature, and time for each sample are given in the following text. After the microwave heating, the stable colloidal solution was obtained. Then 30 mL of ethanol was added to 10 mL of colloidal solution prepared to form a precipitate. The product was filtered, washed with 50 mL of absolute ethanol three times, dried in air at 70 °C for 8 h, and ground to powder by a mortar. The microwave oven (2.45 GHz, maximum power 300 W) used was a focused single-mode microwave synthesis system (Discover, CEM, USA), which was equipped with a magnetic stirrer and a water-cooled condenser. Temperature was controlled by automatically adjusting microwave power.

X-ray powder diffraction (XRD) patterns were recorded with a D/max 2550 V X-ray diffractometer with  $\text{Cu K}\alpha$  radiation ( $\lambda = 1.54178 \text{ \AA}$ ) and a graphite monochromator, operating at 40 kV and 200 mA. Samples were supported on a single-crystalline silicon sample holder. Transmission electron microscopy (TEM) micrographs were taken with a JEOL JEM-2100F field emission transmission electron microscope using an accelerating voltage of 200 kV. For TEM observations, the sample powder was dispersed in ethanol by ultrasonic irradiation, and a drop of the suspension was placed onto a carbon-coated copper grid. The deposit was dried in air prior to observation. Fourier transform infrared (FTIR) spectra were collected on a Nicolet-Nexus Spectrometer, and the KBr disk method was employed. Ultraviolet visible (UV–vis) absorption spectra were obtained with a Techcomp UV2300 spectrophotometer. The sample solutions were diluted by EG, and then put in a quartz cuvette with 1 cm optical path length for measurement. Differential scanning calorimetric analysis (DSC) and thermogravimetric analysis (TG) were carried out with a STA-409PC/4/H Luxx simultaneous TG-DTA/DSC apparatus (Netzsch, Germany) with a heating rate of  $10 \text{ }^\circ\text{C min}^{-1}$  under flowing high-purity  $\text{N}_2$ .

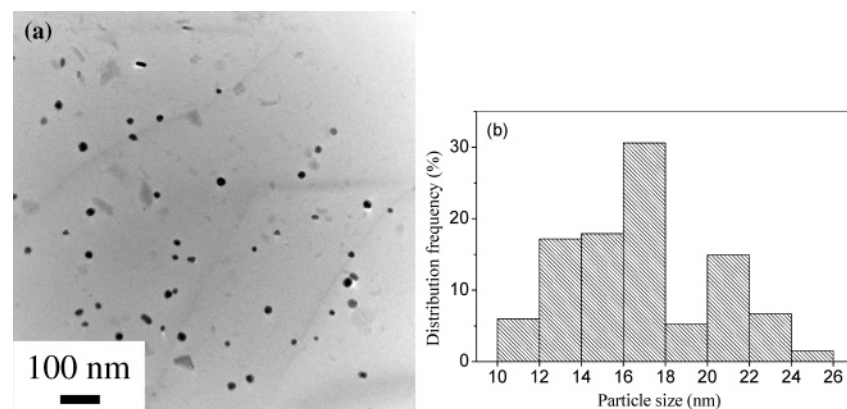
## Results and Discussion

Figure 1a–c shows the XRD patterns for PAM–Ag nanocomposites synthesized at different temperatures. A broad peak centers at about  $23^\circ$ , which is assigned to the PAM polymer phase.<sup>12</sup> All other peaks in XRD patterns can be indexed to a face-centered cubic (fcc) silver (JCPDS No. 4-0783), indicating the formation of PAM–Ag nanocomposite. The broadening of the peak at about  $38^\circ$ , which corresponds to the diffraction of (111) crystal face of silver, indicates that silver particles in the PAM matrix are very small. The crystallite size and crystallinity of silver increased with the reaction temperature, as is clearly illustrated by the more intense and narrow peaks in Figure 1. XRD patterns show that PAM–Pt (Figure 1d) and PAM–Cu (Figure 1e) nanocomposites could also be synthesized by this method. These results suggest that the method reported here is effective to synthesize PAM–metal nanocomposites.

Figure 2a shows the TEM micrograph of the PAM–Ag nanocomposite prepared by microwave heating the EG solution of 0.01 M  $\text{AgNO}_3$  and 3 M AM at 125 °C for 15 min. One can see that spherical Ag nanoparticles were homogeneously dispersed in the polymer matrix. The simultaneous formation of Ag nanoparticles and polymerization of the acrylamide monomer led to a homogeneous distribution of Ag nanoparticles in polyacrylamide matrix. Ethylene glycol acted as both a reducing reagent and a solvent, thus no additional reductant was needed. Another advantage was that no initiator for AM polymerization was necessary. Figure 2b shows the histogram of Ag particle size distribution of the same sample. The diameters of Ag nanoparticles were in the range of 6 to 18 nm, and the average diameter of Ag nanoparticles was  $11.3 \pm 1.9 \text{ nm}$  (1.9 nm is standard deviation), which approximately fits the Gaussian curve. Microwaves resulted in a homogeneous fast heating. Thus  $\text{Ag}^+$  ions were rapidly reduced to  $\text{Ag}^0$  in the whole system, leading to rapid nucleation at the same time, which is a beneficial factor to the formation of nanosized and well-dispersed colloidal Ag nanoparticles. For comparison, the synthesis of PAM–Ag was also conducted in the conventional oil bath. Our experiments showed that the PAM–Ag



**Figure 2.** TEM micrograph (a) and the histogram of Ag particle size distribution (b) of PAM–Ag nanocomposite prepared by microwave heating the EG solution of 0.01 M  $\text{AgNO}_3$  and 3 M AM at 125 °C for 15 min.



**Figure 3.** TEM micrograph (a) and the corresponding particle size histogram (b) of PAM–Ag prepared by oil bath heating the EG solution of 0.01 M  $\text{AgNO}_3$  and 3 M AM at 125 °C for 150 min.

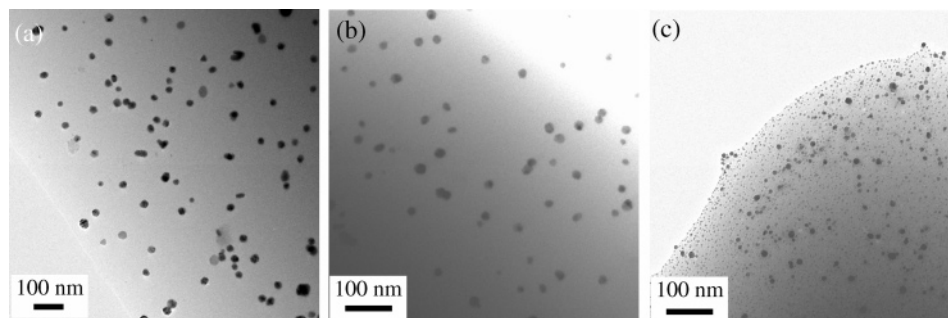


**Figure 4.** TEM micrographs of PAM–Ag nanocomposites prepared by microwave heating the EG solution of  $\text{AgNO}_3$  and 3 M AM: (a) 0.01 M  $\text{AgNO}_3$ , at 190 °C for 15 min; (b) 0.01 M  $\text{AgNO}_3$ , at 125 °C for 45 min; and (c) 0.05 M  $\text{AgNO}_3$ , at 125 °C for 15 min.

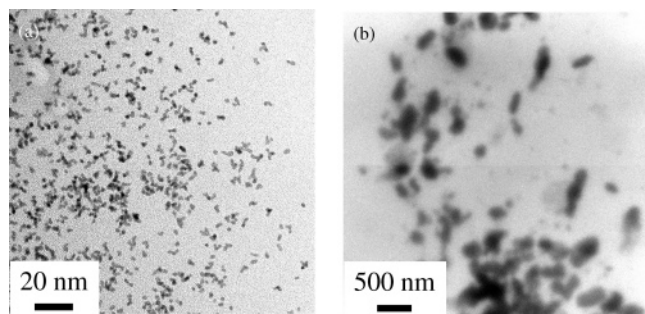
nanocomposite could also be prepared by oil bath at 125 °C; however, much longer reaction time (about 2.5 h) was needed to obtain the PAM–Ag nanocomposite. The average diameter ( $16.9 \pm 3.3$  nm) and size distribution (10–26 nm) of Ag nanoparticles prepared by oil bath for 2.5 h were larger than those prepared by microwave heating at the same temperature with the same reaction solution. The larger Ag nanoparticles obtained by oil bath may result from the longer reaction time and slower Ag nucleation rate.

PAM–Ag nanocomposite with a larger average Ag particle size and a broader particle size distribution was obtained by microwave heating at a higher temperature for 15 min or at 125 °C for a longer reaction time (Figure 4a,b). For example, the average particle size of Ag was  $25.4 \pm 4.3$  nm for the PAM–Ag nanocomposite prepared by microwave heating at 190 °C for 15 min. The average particle size of Ag was  $18.9 \pm 4.4$  nm for the sample prepared by microwave heating at

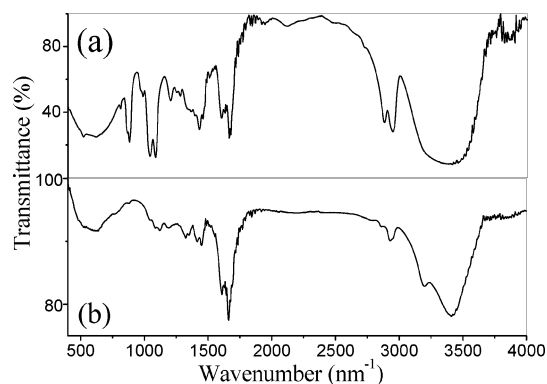
125 °C for 45 min. The larger average Ag particle size and a broader particle size distribution may be ascribed to aggregation and growth of Ag induced by longer reaction time or higher reaction temperature.

Figure 4c shows the TEM micrograph of the PAM–Ag nanocomposite prepared by microwave heating the EG solution of 0.05 M  $\text{AgNO}_3$  and 3 M AM at 125 °C for 15 min. It is obvious that the density of Ag nanoparticles was increased, compared with that of the PAM–Ag nanocomposite prepared by using 0.01 M  $\text{AgNO}_3$ . The average diameter of Ag nanoparticles prepared with 0.05 M  $\text{AgNO}_3$  was  $7.0 \pm 3.9$ , which was smaller than that prepared with 0.01 M  $\text{AgNO}_3$ . However, the Ag particle size distribution prepared with 0.05 M  $\text{AgNO}_3$  was wider than that prepared with 0.01 M  $\text{AgNO}_3$ . This phenomenon can be explained by the influence of  $\text{Ag}^+$  concentration on the nucleation and growth. At higher  $\text{Ag}^+$  concentration, higher concentration of Ag nuclei was formed





**Figure 5.** TEM micrographs of (a) PAM-Pt nanocomposite as in Figure 1d. (b) PAM-Cu nanocomposite as in Figure 1e.



**Figure 6.** FTIR spectra of (a) the EG solution of 0.01 M AgNO<sub>3</sub> and 3 M AM and (b) PAM-Ag nanocomposite prepared by microwave heating the same solution as in part a at 125 °C for 15 min.

at the early stage of nucleation, leading to the formation of more smaller Ag nanoparticles. The nucleation of Ag continued during the Ag crystal growth, resulting in a wider Ag particle size distribution.

TEM images of PAM-Pt and PAM-Cu prepared by the microwave-assisted method are shown in Figure 5. One can see that individual Pt nanoparticles and aggregates are dispersed in PAM, and each aggregate consists of two or three nanoparticles. The diameters of Pt nanoparticles are 1–2 nm. The Cu particle sizes were relatively large in PAM-Cu nanocomposite, about 100–250 nm. The morphologies of Cu particles included sphere, ellipse, rod, and rectangle.

The formation of polyacrylamide in the nanocomposite product was confirmed by the FTIR spectrum in Figure 6. The FTIR spectra of nanocomposites were similar to the standard infrared spectrum of PAM and obviously different from that of the AM monomer.<sup>19</sup> The strong peak at 880 cm<sup>-1</sup> assigned to =CH<sub>2</sub> appears only in the spectrum of the monomer AM (Figure 6a), and vanishes in the spectrum of the nanocomposite (Figure 6b). The strongest peak at 1665.2 cm<sup>-1</sup> ( $\nu$ -C=O) and the characteristic peaks at 2922.3 cm<sup>-1</sup> ( $\nu$ -CH<sub>2</sub>-) and 1454.6 and 1403.9 cm<sup>-1</sup> ( $\delta$ -CH<sub>2</sub>-) of PAM (Figure 6b) further confirm that AM monomer has successfully polymerized under MW irradiation.

To study the stability of the nanocomposite colloidal solution prepared, UV-vis absorption spectra were obtained for the newly prepared sample and after 8 months of storage, as shown in Figure 7a,b. An absorption band centered at around 423 nm was observed due to the surface plasmon resonance of Ag nanoparticles.<sup>20</sup> The UV-vis absorption spectrum of the nanocomposite colloidal solution after aging for 8 months (Figure 7b) was very similar to that of the newly prepared colloidal solution (Figure 7a), suggesting the high stability and nonaggregation of Ag nanoparticles in the nanocomposite colloidal

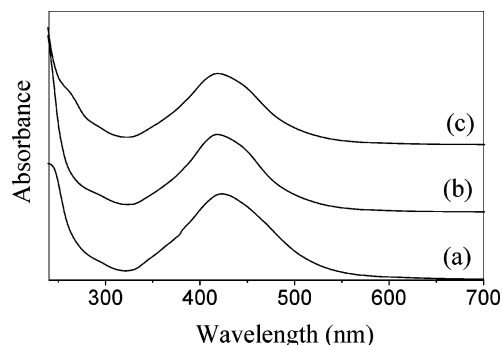


**Figure 7.** UV-vis absorption spectra of (a) a nanocomposite colloidal solution prepared by microwave heating a EG solution of 0.01 M AgNO<sub>3</sub> and 3 M AM at 125 °C for 15 min; (b) after 8 months aging of colloidal solution from part a; and (c) the redispersed nanocomposite colloidal EG solution.

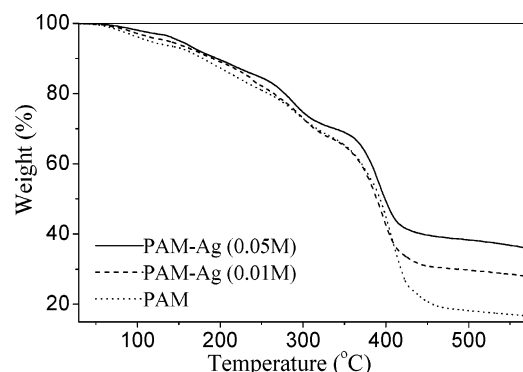


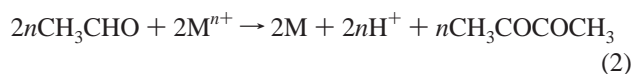
**Figure 8.** TG analysis of pure PAM and PAM-Ag nanocomposites with different Ag content prepared by microwave heating at 125 °C for 15 min.

solution. In addition, the nanocomposite powder collected from the colloidal solution could be easily redispersed in EG to form the stable colloid by simple agitation for a few minutes. The UV-vis absorption spectrum of redispersed colloidal solution (Figure 7c) was also very similar to that of the newly prepared one, implying that Ag nanoparticles do not aggregate after a cycle of drying to powder and redispersion in EG. This is important for convenient storage and transportation of the nanocomposite materials.

TG curves of pure PAM and PAM-Ag nanocomposites are given in Figure 8. Three stages of weight loss can be observed in all cases. The first slow weight loss below 250 °C can be assigned to the loss of absorbed water in PAM.<sup>21</sup> The second loss between 250 and 330 °C may correspond to the evolution of NH<sub>3</sub>.<sup>22</sup> The last weight loss appears sharply above 350 °C due to the pyrolysis of the imides formed during the second stage.<sup>23</sup> After the TG measurement, a black residue was left. In Figure 8, the residual mass curve with low Ag concentration is a little lower than or leftward to that with high Ag concentration. In other words, the pyrolysis of the same amount of PAM requires a little higher temperature for the sample with higher Ag concentration. This result implies that the thermal stability of PAM can be slightly enhanced by the presence of a small amount of Ag as nanofiller. It is interesting to point out that the residual weight of the nanocomposite at 600 °C was much higher than the total amount of the residual weight of pure PAM and the embodied Ag, that is to say, the residual weight of PAM was increased due to the presence of a small quantity of Ag nanoparticles. The different residual weights between pure PAM and PAM-Ag nanocomposites may be another proof of the improvement of the thermal stability of PAM by Ag nanopar-

ticles. The similar results were also reported for polystyrene–CdS<sup>24</sup> and polyvinyl alcohol–Ag composites.<sup>25</sup>

In this work, polymerization of AM was carried out in EG. The C=C bond in the AM monomers readily absorb the microwave energy to form excited-state monomer M\*, and then decompose to radicals, leading to polymerization. This process can be facilitated in the EG solvent, which has a high dielectric loss constant (41.0) to absorb microwave efficiently. EG also serves as a reductant for the formation of metal under MW irradiation. The metallic nanoparticles can be produced by the following reactions:<sup>26</sup>



The high viscosity of the system due to the polymerization of AM prevents the movement, growth, and aggregation of nanosized metal. On the other hand, PAM that contains the O=C–N group is easily attached to the surface of the nanocrystal metal, which lowers the surface free energy of nanosized metal, stabilizes it, and restrains its growth and aggregation. Hence in this work, the product PAM also acts as a stabilizer. While in other cases, PVP or another surfactant is indispensable for the preparation of uniform Ag or other metal nanoparticles in EG by MW.<sup>18,27</sup>

## Conclusion

In summary, microwave heating provides a convenient and efficient method for in situ single-step synthesis of PAM–metal nanocomposites. This novel technique is based on the simultaneous formation of the colloidal metal nanoparticles and the polymerization of the acrylamide monomer in solution. Nanosized metal particles with a narrow size distribution can be homogeneously dispersed in the PAM matrix. EG acts as a solvent, a reducing reagent, and a microwave absorber at the same time. No additional initiator, surfactant, and stabilizer are necessary in the synthesis, which benefits to the low-cost production of high-purity product. As compared to pure PAM, PAM–Ag nanocomposites have improved thermal stability. This novel method is expected to be extended to synthesize other polymer–metal nanocomposites.

**Acknowledgment.** This work was funded by National Natural Science Foundation of China (50472014), the Chinese

Academy of Sciences under the Program for Recruiting Outstanding Overseas Chinese (Hundred Talents Program), the Fund for Innovation Research from Shanghai Institute of Ceramics, the Chinese Academy of Sciences, the K. C. Wong Education Foundation of Hong Kong, the Program of Shanghai Postdoctoral Scientific Research Foundation (05R214148), the fund from the State Key Laboratory of High Performance Ceramics and Superfine Microstructure (SKL200506SIC), the Shanghai Institute of Ceramics, Chinese Academy of Sciences.

## References and Notes

- (1) Dirix, Y.; Bastiaansen, C.; Caseri, W.; Smith, P. *J. Mater. Sci.* **1999**, *34*, 3859.
- (2) Caseri, W. *Macromol. Rapid Commun.* **2000**, *21*, 705.
- (3) Shiraishi, Y.; Toshima, N. *Colloids Surf. A* **2000**, *169*, 59.
- (4) Sarma, T. K.; Chowdhury, D.; Paul, A.; Chattopadhyay, A. *Chem. Commun.* **2002**, 1048.
- (5) Schurmann, U.; Hartung, W.; Takele, H.; Zaporozhchenko, V.; Faupel, F. *Nanotechnology* **2005**, *16*, 1078.
- (6) Dirix, Y.; Bastiaansen, C.; Caseri, W.; Smith, P. *Adv. Mater.* **1999**, *11*, 223.
- (7) Sarkar, A.; Kapoor, S.; Yashwant, G.; Salunke, H. G.; Mukherjee, T. *J. Phys. Chem. B* **2005**, *109*, 7203.
- (8) Nakao, Y. *J. Chem. Soc., Chem. Commun.* **1993**, 826.
- (9) Watkins, J. J.; McCarthy, T. J. *Chem. Mater.* **1995**, *7*, 1991.
- (10) Ye, S. Y.; Vijh, A. K.; Wang, Z. Y.; Dao, L. H. *Can. J. Chem.* **1997**, *75*, 1666.
- (11) Warshawsky, A.; Upson, D. A. *J. Polym. Sci., Part A: Polym. Chem.* **1989**, *27*, 2995.
- (12) Zhu, Y. J.; Qian, Y. T.; Li, X. J.; Zhang, M. W. *Chem. Commun.* **1997**, 1081.
- (13) Yin, Y. D.; Xu, X. L.; Xia, C. J.; Ge, X. W.; Zhang, Z. C. *Chem. Commun.* **1998**, 941.
- (14) Zhou, Y.; Yu, S.; Wang, C.; Zhu, Y.; Chen, Z. *Chem. Lett.* **1999**, 677.
- (15) Zhang, Z.; Han, M. *J. Mater. Chem.* **2003**, *13*, 641.
- (16) Kappe, C. O. *Angew. Chem., Int. Ed.* **2004**, *43*, 6250.
- (17) Roberts, B. A.; Strauss, C. R. *Acc. Chem. Res.* **2005**, *38*, 653.
- (18) Tsuji, M.; Hashimoto, M.; Nishizawa, Y.; Kubokawa, M.; Tsuji, T. *Chem. Eur. J.* **2005**, *11*, 440.
- (19) Sprouse, J. F.; Hansen, D. L., Eds. *Sprouse Collection of Infrared Spectra Book I: Polymers 357*; Sprouse Scientific Systems: Paoli, PA, 1987; Standard Infrared Grating Spectra, Vols. 9–10 (8001–10000), 8284.
- (20) Creighton, J. A.; Eadon, D. G. *J. Chem. Soc., Faraday Trans.* **1991**, *87*, 3881.
- (21) Rangaraj, A.; Vangani, V.; Rakshit, A. K. *J. Appl. Polym. Sci.* **1997**, *66*, 45.
- (22) Yang, M. H. *Polym. Test.* **1998**, *17*, 191.
- (23) Yang, M. H. *J. Appl. Polym. Sci.* **2002**, *86*, 1540.
- (24) Šajinović, D.; Šaponjić, Z. V.; Cvjetičanin, N.; Marinović-Cincović, M.; Nedeljković, J. M. *Chem. Phys. Lett.* **2000**, *329*, 168.
- (25) Mbhele, Z. H.; Salemane, M. G.; van Sittert, C. G. C. E.; Nedeljković, J. M.; Djoković, V.; Luyt, A. S. *Chem. Mater.* **2003**, *15*, 5019.
- (26) Fievet, F.; Lagier, J. P.; Blin, B.; Beaudoin, B.; Figlarz, M. *Solid State Ionics* **1989**, *32/33*, 198.
- (27) Komarneni, S.; Li, D.; Newalkar, B.; Katsuki, H.; Bhalla, A. S. *Langmuir* **2002**, *18*, 5959.